energies

MDPI

Article

Design and Hardware Implementation Based on Hybrid Structure for MPPT of PV System Using an Interval Type-2 TSK Fuzzy Logic Controller

O. Fatih Kececioglu *, Ahmet Gani and Mustafa Sekkeli

Department of Electrical and Electronics Engineering, Kahramanmaras Sutcu Imam University, 46050 Kahramanmaras, Turkey; agani@ksu.edu.tr (A.G.); msekkeli@ksu.edu.tr (M.S.)

* Correspondence: fkececioglu@ksu.edu.tr; Tel.: +90-344-300-1639

Received: 1 February 2020; Accepted: 8 April 2020; Published: 10 April 2020

Abstract: The major drawback of photovoltaic (PV) systems is their dependence on environmental conditions, such as solar radiation and temperature. Because of this dependency, maximum power point tracking (MPPT) control methods are used in PV systems in order to extract maximum power from the PV panels. This study proposes a controller with a hybrid structure based on angle of incremental conductance (AIC) method and Interval Type-2 Takagi Sugeno Kang fuzzy logic controller (IT2-TSK-FLC) for MPPT. MPPT performance of proposed hybrid controller is evaluated via detailed simulation studies and dSPACE-based experimental study. The results validate that the proposed hybrid controller offers fast-tracking speed, high stability, and robust performance against uncertainties arising from disturbance to inputs of the PV system.

Keywords: MPPT; Interval Type-2 TSK fuzzy logic controller; AIC

1. Introduction

Photovoltaic (PV) power generation has become very widespread throughout the world, because of its advantages such as lesser maintenance, absence of moving parts, which eliminates the noise effect, low cost, and increasing efficiency of the equipment in PV systems (such as power electronic converters). However, the major drawback of PV systems is their high dependence on solar irradiance and temperature [1]. Current-Voltage (I-V) and Power-Voltage (P-V) characteristic curves of PV panels are non-linear. There is an optimum power point called the maximum power point (MPP) on the curves, and a PV panel generates maximum output power at the MPP. In addition, the MPP on the characteristics curve is influenced by solar irradiance and temperature. To extract maximum available power from a PV panel, a DC-DC converter is controlled by the maximum power point tracking (MPPT) method in order to operate the panel at MPP [2].

To date, various studies have been conducted aiming to increase the efficiency of the MPPT methods on PV systems.

Tian et al. [3] presented a modified asymmetrical variable step size incremental conductance (INC) MPPT method that is based on the asymmetrical feature of the P-V curve. The proposed algorithm compared with the conventional fixed or variable step size method. The authors stated that the proposed algorithm improved tracking accuracy and speed. Soon and Mekhilef [4] proposed a simpler fast-converging maximum power point tracking technique which used the relationship between the load line and the I-V curve. The results were compared with the conventional INC MPPT method and it was shown that the proposed algorithm was four times faster than the conventional INC MPPT method during the load and solar irradiation variation. Dogmus et al. [5] proposed an MPPT algorithm with proportional-integral-derivative (PID) optimization based on particle swarm optimization (PSO)

for single MPP PV systems, in order to increase the performance of the perturb and observe (P&O) MPPT algorithm. The proposed MPPT algorithm was compared with a conventional PID controller and the P&O MPPT algorithm in order to test its tracking performance for MPP. The authors stated that the tracking performance of MPP increased from 96.7% to 99.0%.

Loukriz et al. [6] proposed a new variable step size incremental conductance (INC) MPPT method. Under similar operating conditions, INC MPPT methods with variable step size and fixed step size were compared. Comparative results showed that the proposed method tracks the maximum power point with less power oscillation. Liu et al. [7] proposed a modified variable step size INC MPPT method that automatically adjusts the step size for MPP. The proposed method was compared with the classical fixed step size method. The proposed method has simultaneously improved the MPP tracking speed and tracking accuracy.

Kececioglu et al. [8] proposed a Type-1 fuzzy–PI controller for maximum power point tracking. To validate the performance of proposed controller, a simulation model was realized by using the Matlab/Simulink environment. The proposed controller was compared with the conventional PI controller. The proposed Type-1 fuzzy-PI controller has superior performance compared to a conventional PI controller under varying atmospheric conditions.

Yilmaz et al. [9] improved a new MPPT method using adapting calculation based on Type-1 fuzzy logic controller. The proposed MPPT method tested by the simulations on Matlab/Simulink under variable atmospheric conditions and compared with the performance of the P&O, INC, and conventional FLC respectively. The authors concluded that the proposed MPPT method has better performance than other methods to determine MPP. Palaniswamy and Srinivasan [10] presented a Takagi-Sugeno (T-S) fuzzy-based MPPT algorithm for a standalone photovoltaic system. The algorithm presented was validated using Matlab/Simulink under various operating conditions and compared to the INC algorithm. The authors stated that the effectiveness of the proposed T-S fuzzy algorithm in tracking maximum power was better than the INC algorithm. Rezk et al. [11] proposed an adaptive Type-1 fuzzy logic controller-based new MPPT methodology for controlling PV systems. The authors emphasized that main advantage in the proposed method is accurate and adaptive tracking performance of the operating maximum power extraction point of the PV system, and the mitigation of power fluctuations in transient and steady state operating points. Ozdemir et al. [12] presented a Type-1 fuzzy logic based MPPT method for quadratic boost converter. The method presented was validated by using simulation and experimental studies. Altin [13] presented an MPPT method based on an Interval Type-2 fuzzy logic controller. The author tested the proposed method using Matlab/Simulink and stated that the proposed method provides fast dynamic response under rapidly changing atmospheric conditions.

Danandeh and Mousavi [14] proposed a hybrid MPPT method based on Type-1 fuzzy logic that is combined with the INC algorithm. The proposed hybrid MPPT method was tested under standard and changing conditions, and compared with the conventional Type-1 fuzzy logic controller and INC algorithm. Results showed that the proposed hybrid MPPT method exhibits good behavior under stable and fast-changing conditions. Shiau et al. [15] presented a comparative study on fuzzy logic-based solar power MPPT algorithms using different fuzzy input variables. The authors concluded that the range of the input variable of the angle of incremental conductance (AIC) algorithm is finite and the maximum power point condition is well defined in a steady condition and, therefore, it can be used for multipurpose controller design.

When the literature on MPPT methods based on the fuzzy logic controller was examined, it was observed that the Interval Type-2 Takagi Sugeno Kang fuzzy logic controller (IT2-TSK-FLC) and AIC MPPT algorithm have not been combined for this purpose, despite the advantages of the AIC MPPT algorithm and Interval Type-2 Takagi Sugeno Kang (TSK) fuzzy logic system. In this paper, a hybrid control structure that is called AIC-IT2-TSK-FLC, based on the AIC MPPT algorithm and Interval Type-2 Takagi Sugeno Kang fuzzy logic controller is proposed for the MPPT of a PV system.

The main contributions of this study are listed below:

- A new intelligent hybrid controller that is combined AIC MPPT algorithm and Interval Type-2 TSK fuzzy logic controller is proposed.
- The AIC algorithm is selected to generate the error function of Interval Type-2 TSK fuzzy logic controller.
- Interval Type-2 TSK fuzzy logic controller is preferred to handle the uncertainties in solar irradiances and temperature.
- The exact duty cycle of the DC-DC converter is adjusted by proposed hybrid controller.
- The proposed hybrid controller is studied under stringent solar irradiances and temperature profiles via detailed simulation and experimental studies.
- The proposed hybrid controller can handle as possible abnormal conditions and improves the efficiency, tracking accuracy, and reduce the steady-state power oscillation.
- Unlike many existing MPPT methods, the proposed hybrid controller has high adaptation ability for a new operating point at any time.

The present paper is organized as follows. The proposed hybrid control structure is given in Section 2. The dynamic performance of the AIC MPPT method and proposed hybrid controller are compared with detailed simulation studies in Section 3. The dynamic performance of the proposed hybrid controller is analyzed with experimental studies in Section 4. Finally, the conclusions of the study are explained in Section 5.

2. Proposed Hybrid Control Structure

Introduced by Lotfi A. Zadeh in 1975, Type-2 fuzzy sets are an extension of Type-1 fuzzy sets. A Type-1 fuzzy set with x ∈ X and a single variable can be represented as follows:

$$A = (x, \mu_A(x)) \mid \forall x \in X, \mu_A(x) \in [0, 1] \quad (1)$$

The Type-1 fuzzy set given in Equation (1) does not have any uncertainties. In other words, each x input has a certain membership value between 0–1. If the membership degree of a variable is not known, a Type-2 membership function should be used instead [16]. Type-1 and Type-2 Gaussian fuzzy sets are shown in Figure 1.

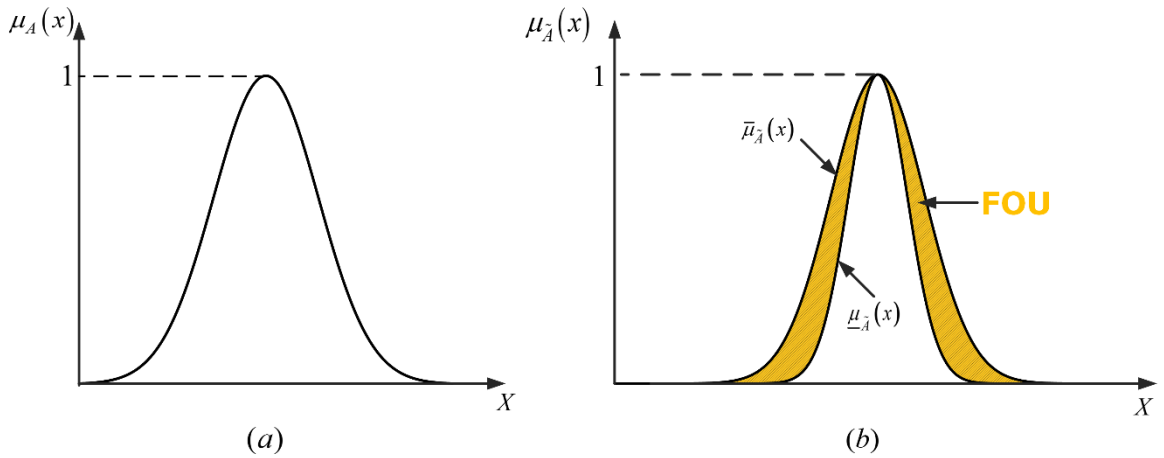

Figure 1. Gaussian fuzzy sets of Type-1 (**a**) and Type-2 (**b**).

Fuzzy logic control (FLC) is a widely-used method to perform MPPT for the PV system. Numerous studies [17–24] in the existing literature have demonstrated that Type-1 FLC (T1FLC) does not succeed in highly uncertain situations in the system, while a Type-2 FLC using Type-2 fuzzy set display better performance. In the present paper, a hybrid control structure called AIC-IT2-TSK-FLC was developed

for MPPT of the PV system with a combination of the AIC MPPT algorithm and Type-2 FLC [25]. The proposed hybrid control structure is shown in Figure 2.

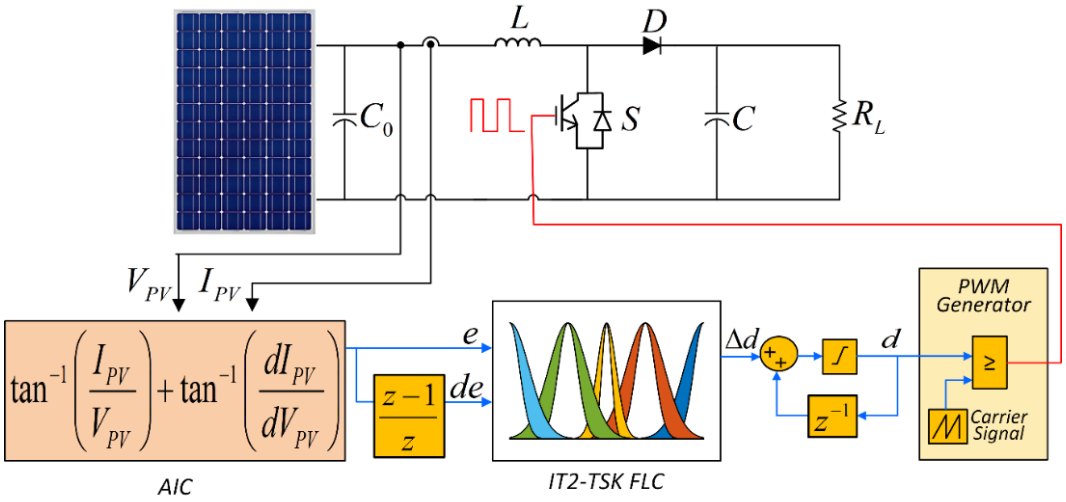

Figure 2. Proposed hybrid control structure.

It can be seen Figure 2 that the proposed hybrid control structure was applied to the PV system consisting of a PV panel and DC-DC power converter. The boost converter topology was selected in this study. Instantaneous voltage (V_{PV}) and current (I_{PV}) were measured on the PV panel using voltage and current sensors. The AIC MPPT algorithm was used to generate the error function of IT2-TSK-FLC responsible for the minimization of the error of MPP. The rate of change in the duty cycle (Δd) was provided by the IT2-TSK-FLC. The rate of change value of the duty cycle was summed with its previous value, in order to obtain the duty cycle of the converter (d). The output of the proposed hybrid control structure was applied to the switching device in the DC-DC boost converter. The control signal, which is the output of IT2-TSK-FLC, was generated using Type-2 fuzzy sets. A Type-2 fuzzy set consists of triples (x,u):$\mu_{\widetilde{A}}(x,u)$ where x ∈ X, a primary membership value, u ∈ J_x (J_x is the range of primary membership for a given x) and a secondary membership, $\mu_{\widetilde{A}}(x,u)$, for each member of domain, can be defined as follows:

$$\widetilde{A} = \left\{\left((x,u),\mu_{\widetilde{A}}(x,u)\right)\middle|\forall x \in X,\ \forall u \in J_x \subseteq [0,1], \mu_{\widetilde{A}}(x,u) \in [0,1]\right\} \quad (2)$$

The footprint of uncertainty (FOU) shown in Figure 3 is the limited domain representing the primary uncertainty of the Type-2 fuzzy set between upper ($\overline{\mu}_A$) and lower ($\underline{\mu}_A$) membership functions. The FOU domain between upper and lower membership functions in the Type-2 fuzzy set was assumed to be an infinite Type-1 membership function. While general Type-2 fuzzy sets preserve their main properties, interval Type-2 fuzzy sets are introduced as an alternative in order to reduce the computational burden [26]. When all $\mu_{\widetilde{A}}(x,u)$ is equal to 1, $\widetilde{A}$ is an Interval Type-2 fuzzy set. Interval Type-2 fuzzy sets can be defined as follows:

$$\widetilde{A} = \{((x,u),1)\,|\,\forall x \in X, \forall u \in J_x \subseteq [0,1]\} \quad (3)$$

Both general and Interval Type-2 fuzzy logic membership functions are three dimensional. The only difference between them is that the secondary membership function value of an Interval Type-2 fuzzy logic function is equal to 1. Therefore, the computational time of these sets is shorter compared to the general Interval Type-2 fuzzy logic controller (IT2-FLC). IT2-FLC consists of four main parts: fuzzification, rule base, fuzzy inference, and type reducer [27]. The main difference between IT2-FLC and the Type-1 fuzzy logic controller is type reduction. Type-2 fuzzy sets can be converted to Type-1 fuzzy sets thanks to type reduction. The output of the type reduction block is a Type-1 fuzzy set. All of

the Type-1 fuzzy sets obtained were converted to crisp outputs thanks to the defuzzifier. The internal structure of IT2-TSK-FLC is shown in Figure 4.

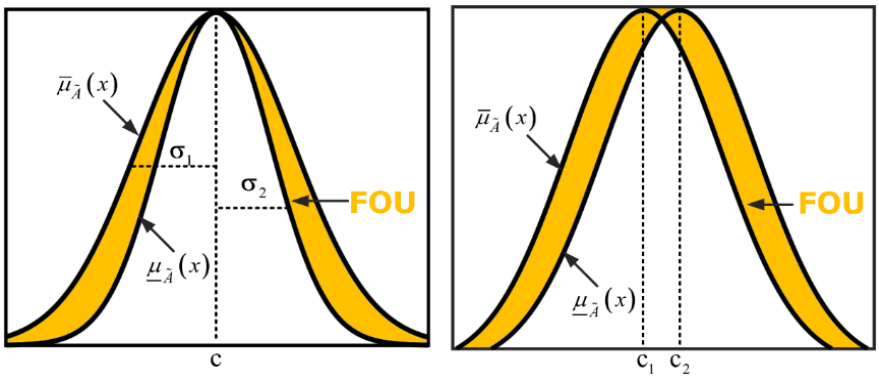

Figure 3. Gaussian Type-2 fuzzy set.

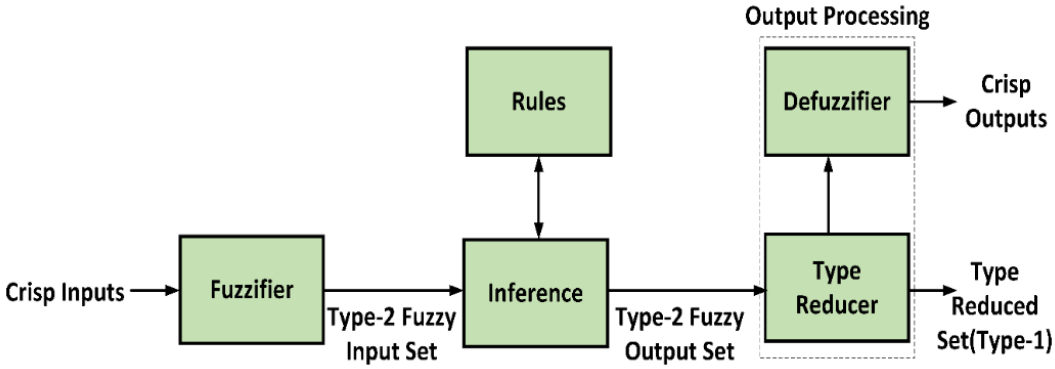

Figure 4. The internal structure of the Interval Type-2 Takagi Sugeno Kang fuzzy logic controller (IT2-TSK-FLC).

As shown in Figure 4, crisp inputs were fuzzified with Type-2 input membership functions, then the fuzzy inference engine generated the controller signal according to the input values, membership functions, and rule base. After the type reducing and defuzzifying processes, crisp values of the IT2-TSK-FLC were obtained. The proposed IT2-TSK-FLC inference mechanism was defined in three different models as A2-C1, A2-C0, and A1-C1. The A2-C0 TSK model was used in the inference mechanism of IT2-TSK-FLC in the present study. The antecedents are Type-2 fuzzy sets, while the consequents are first-order polynomials in the A2-C0 TSK model. The A2-C0 TSK model can be defined by fuzzy If-Then rules [28]. The A2-C0 TSK rule base can be defined as follows:

$$R^k : IF \;\; x_1 \;\; is \;\; \widetilde{A}_1^j \;\; AND \;\; x_2 \;\; is \; \widetilde{A}_2^n \;\; THEN \;\; LF_k = p_k x_1 + q_k x_2 + r_k \tag{4}$$

where k = 1,2, ...,25 represents rule numbers; x_1, x_2 are input variables (e, de); $\widetilde{A}_1^j$ and $\widetilde{A}_2^n$ are membership functions; LF_k is the rule output; p_k, q_k, r_k are the consequent parameters. Gaussian type membership functions are preferred due to their smoothness and nonzero at all points on the control algorithm. This also will affect the power accuracy of systems under the steady-state response. [29]. For that reason, the Gaussian type membership function was selected. The mathematical equations for the Gaussian type membership function are given in Equations (5) and (6).

$$\overline{\mu}_{\widetilde{A}_i^j}(x_i) = \exp\left\{-\frac{1}{2}\left(\frac{x_i - c_{ij}}{\overline{\sigma}_{ij}}\right)^2\right\} \tag{5}$$

$$\underline{\mu}_{\underline{\tilde{A}}_i^j}(x_i) = \exp\left\{-\frac{1}{2}\left(\frac{x_i - c_{ij}}{\underline{\sigma}_{ij}}\right)^2\right\} \tag{6}$$

where $\mu_{\tilde{A}_i^j}(x_i)$ denotes the degree of membership for input variable, represents the mean value of function, is standard deviation and x_i is the input variable [30]. IT2-TSK-FLC has two inputs (e, de) and single output (Δd) which is rate change of duty cycle for DC-DC converter.

Design Specifications of Interval Type-2 TSK-FLC

The detailed structure of IT2-TSK-FLC is shown in Figure 5. As shown in Figure 5, the IT2-TSK-FLC configuration consists of seven layers.

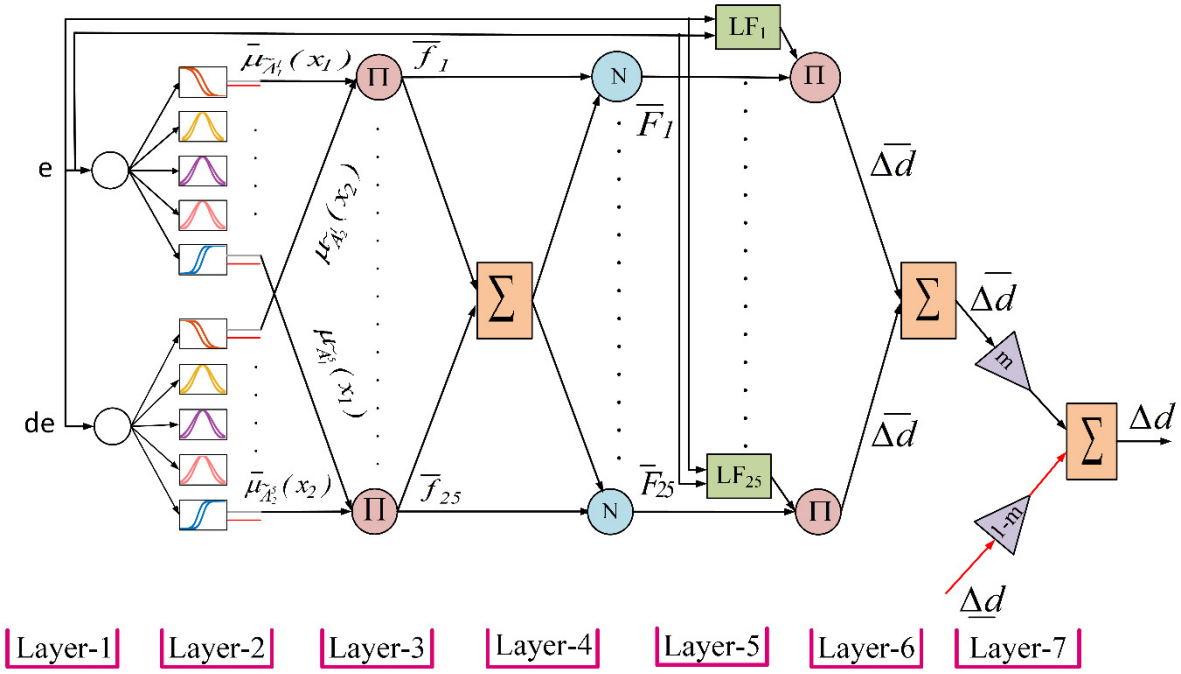

Figure 5. Structure of IT2-TSK-FLC.

Layer-1: This layer is the input layer. As seen in Figure 1, the inputs of controller (e, de) is generated by the AIC MPPT algorithm, described in Equation (7). The characteristic curves of the AIC MPPT algorithm are shown in Figure 6. As seen in Figure 6, the angle is equal to zero around the MPP point.

$$\tan^{-1}\left(\frac{I_{pv}}{V_{pv}}\right) + \tan^{-1}\left(\frac{dI_{pv}}{dV_{pv}}\right) = 0 \tag{7}$$

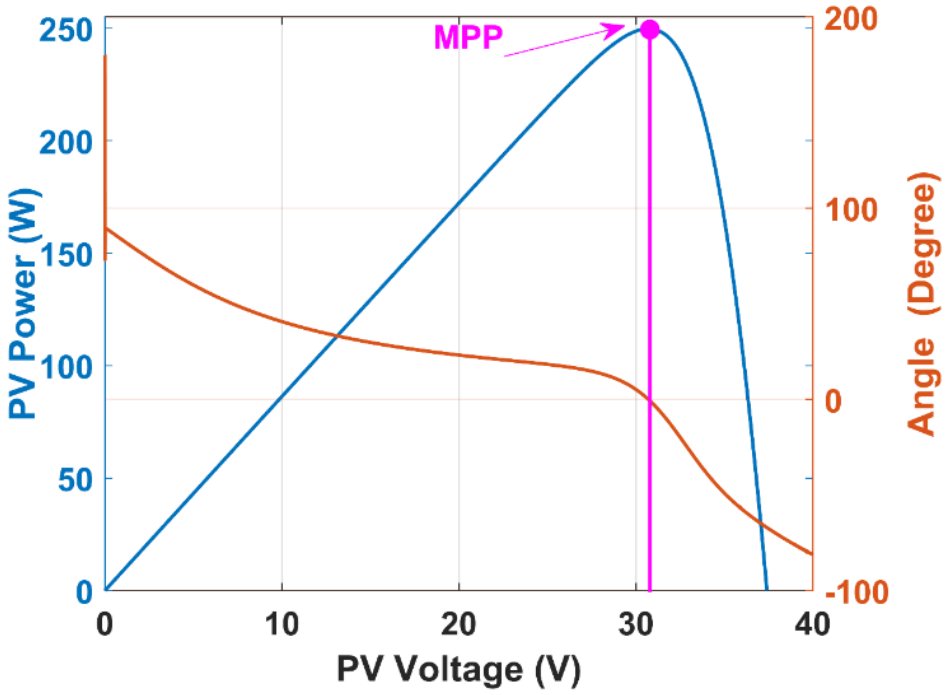

Figure 6. Angle of incremental conductance (AIC) angle curve and photovoltaic (PV) panel power versus voltage characteristic curves.

Layer-2: In this layer, the degrees of the membership functions are determined for inputs. The membership functions of the input and the rule base of the proposed hybrid control structure must be identified according to the MPP condition for the IT2-TSK fuzzy inference system. The membership functions are labeled with negative big (NB), negative small (NS), zero (ZE), positive small (PS), and positive big (PB). The membership functions are determined for error (e) and change of error (de) of the proposed hybrid control structure. Input membership functions are scaled to the range (−1, +1). Five gaussian membership functions designed for the inputs are shown in Figure 7.

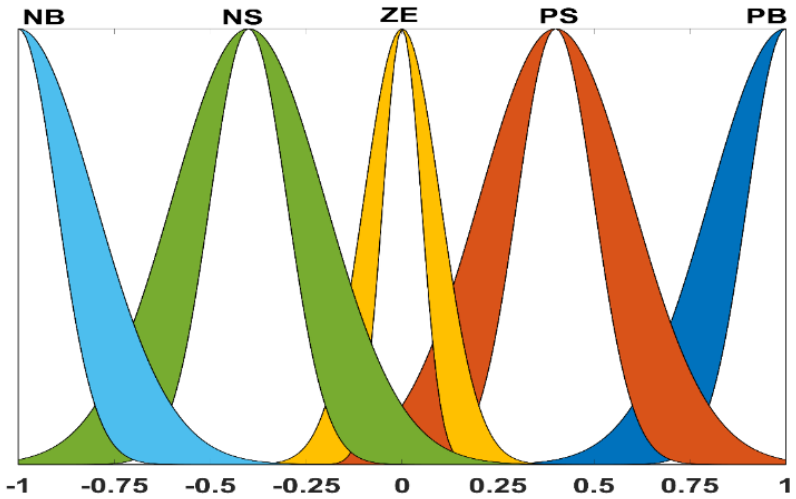

Figure 7. Five gaussian membership functions designed for inputs.

Layer-3: The third layer of the IT2-TSK-FLC consists of the nodes indicated by Π. The firing strengths of the fuzzy rules are defined as lower and upper using the product operator. The fuzzy rules

of the proposed hybrid control structure are given Table 1. The mathematical equations of Layer-3 are given below:

$$\overline{f}_{(n-1)\times J+j} = \overline{\mu}_{\widetilde{A}_1^j}(x_1) * \overline{\mu}_{\widetilde{A}_2^n}(x_2) n = 1, 2, \ldots, N \text{ and } k = (n-1) \times J + j \tag{8}$$

$$\underline{f}_{(n-1)\times J+j} = \underline{\mu}_{\underline{\widetilde{A}}_{j}}(x_1) * \underline{\mu}_{\underline{\widetilde{A}}_{n}}(x_2) n = 1, 2, \ldots, N \text{ and } k = (n-1) \times J + j \tag{9}$$

Table 1. Fuzzy rules of proposed hybrid control structure.

Δd	de					
		NB	**NS**	**ZE**	**PS**	**PB**
e	NB	LF1	LF2	LF3	LF4	LF5
	NS	LF6	LF7	LF8	LF9	LF10
	ZE	LF11	LF12	LF13	LF14	LF15
	PS	LF16	LF17	LF18	LF19	LF20
	PB	LF21	LF22	LF23	LF24	LF25

NB: Negative Big, NS: Negative Small, ZE: Zero, PS: Positive Small, PB Positive Big, LF: Linear Function.

Layer-4: This layer is also known as the normalization layer, and each node is labeled as N. Normalization is performed by proportioning the firing strength of each node rule to the sum of the firing strengths of all rules. The normalization process is defined as follows:

$$\overline{F_k} = \frac{\overline{f_k}}{\sum \overline{f_k}} \qquad k = 1, 2, \ldots, 25 \tag{10}$$

$$\underline{F_k} = \frac{\underline{f_k}}{\sum \underline{f_k}} \qquad k = 1, 2, \ldots, 25 \tag{11}$$

Layer-5: This is a linear function (LF) layer. The LF outputs are calculated according to the rule base. Layer outputs are computed as follows:

$$LF_k = p_k e + q_k de + r_k \qquad k = 1, 2, \ldots, 25 \tag{12}$$

Layer-6: The multiplication of membership degrees for upper and lower membership functions and linear functions are obtained in this layer.

$$\overline{\Delta d} = \prod_{k=1}^{25} \overline{F_k LF_k} \tag{13}$$

$$\underline{\Delta d} = \prod_{k=1}^{25} \underline{F_k LF_k} \tag{14}$$

Layer-7: Biglarbegian-Melek-Mendel (BMM) method is a closed-form type reduction and defuzzification method used in this layer [31]. The closed mathematical form of type reduction and defuzzification process for the proposed hybrid controller are calculated as follows:

$$\Delta d = m \frac{\sum_{k=1}^{25} \overline{f_k LF_k}}{\sum_{k=1}^{25} \overline{f_k}} + (1-m) \frac{\sum_{k=1}^{25} \underline{f_k LF_k}}{\sum_{k=1}^{25} \underline{f_k}} \tag{15}$$

3. Simulation Studies

In this section, we describe the simulation of the proposed hybrid controller for MPPT using the MATLAB/Simulink environment and Sim Power System Toolbox. To evaluate the performance of the proposed hybrid controller under the various environmental conditions, simulation studies were also performed under different operation conditions, described as follows:

Case 1: In this case, solar irradiance and panel temperature values were set to standard test condition (STC) values of 1000 W/m^2 and 25 °C. Thus, steady state and transient performances of the proposed hybrid controller were evaluated for STC.

Case 2: In this case, the performance of the proposed hybrid controller was analyzed against input disturbance under extreme environmental conditions.

3.1. PV System and Converter Modelling

A PV panel that had a single MPP was used for PV simulation modeling. The MPP value of the PV panel at the STC was 250 W. Electrical characteristic parameters of the PV panel are listed in Table 2. The DC-DC converter values selected for simulation studies are given in Table 3. The modeled system using MATLAB/Simulink is shown in Figure 8.

Table 2. Electrical characteristic parameters of a PV panel.

Panel Type	Polycrystalline	
Optimum Operating Voltage	V_{MP}	30.7 V
Optimum Operating Current	I_{MP}	8.15 A
Open – Circuit Voltage	V_{oc}	37.4 V
Short – Circuit Current	I_{sc}	8.63 A
Maximum Power at STC	P_{max}	250 W
Panel Efficiency	η	15.4%

Table 3. DC-DC converter parameters.

Inductor	L	10 mH
Capacitor	C_0	330 µF
Capacitor	C	220 µF
Load Resistance	R_L	40 Ω
Switching Frequency	f	20 kHz

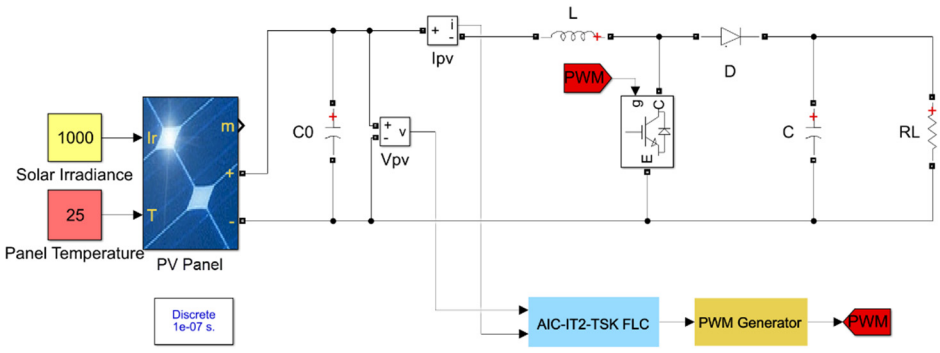

Figure 8. Simulation model.

3.2. Simulation Results

3.2.1. Case 1

In this part of the simulation studies, the performance of the proposed hybrid controller was analyzed under STC. Simulation results for output power of a PV panel and DC-DC converter obtained

from AIC-IT2-TSK-FLC were compared with conventional AIC MPPT method and AIC Type-1 TSK-FLC (AIC-T1-TSK-FLC), which is one of the existing fuzzy control methods

Total simulation time was 0.1 s for this case. Simulation results are shown in Figure 9. It can be noted that the settling times of the proposed hybrid control structure, AIC-T1-TSK-FLC, and AIC MPPT method were 5 ms, 20 ms, and 52 ms respectively. Maximum power extracted from the PV panel of the proposed hybrid controller, AIC-T1-TSK-FLC hybrid controller, and conventional AIC MPPT method following the settling times were 249.6 W, 248.9 W, and 248.2 W respectively.

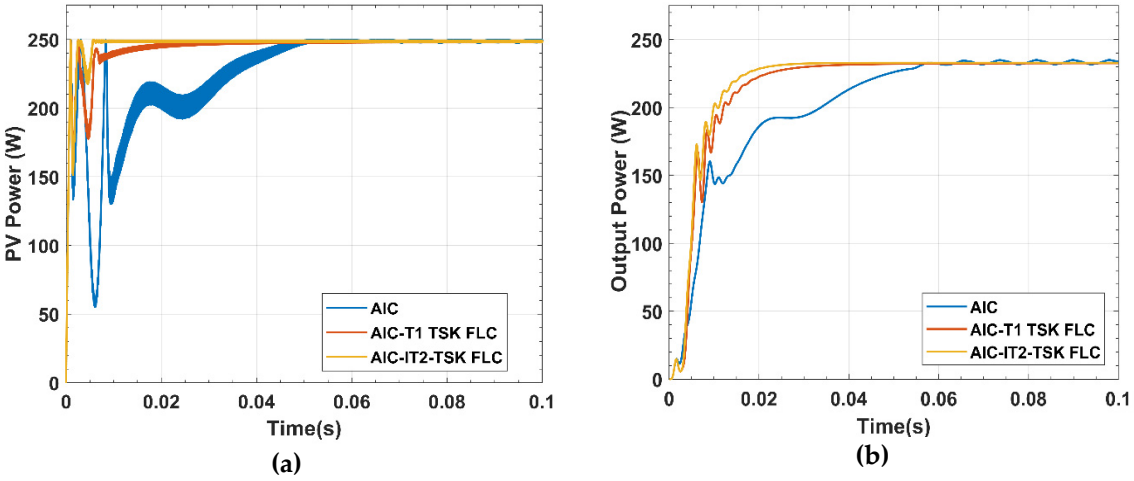

Figure 9. Output power responses of PV panel (**a**) and converter (**b**) for Case 1.

As shown in Figure 9b, DC-DC converter output powers of IT2-TSK-FLC, AIC-T1-TSK-FLC, and AIC MPPT were 232.9 W, 231.5 W, and 230.3 W respectively. It is evident that unlike the conventional AIC MPPT method, the proposed hybrid control structure was reduced to oscillation on the PV panel and converter output power. According to converter design considerations, the power conversion efficiency of the DC-DC converter was equal to 93.31%, which is acceptable for boost converter design.

Performance comparison of all MPPT controllers are presented in terms of performance parameters in Table 4.

Table 4. Performance comparison of all maximum power point tracking (MPPT) controllers.

Parameters	AIC-IT2-TSK-FLC	AIC-T1-TSK-FLC	AIC
Maximum PV Power	249.6 W	248.9 W	248.2 W
Power Conversion Efficiency	93.31%	92.93%	92.78%
Tracking Accuracy	99.84%	99.55%	99.28%

3.2.2. Case 2

This case was separated into six states in order to evaluate the performance of the proposed hybrid controller against extreme environmental conditions. At the first state, solar irradiance and panel temperature values were fixed at 1000 W/m^2 and 25 °C, respectively. In the second state of the case, the solar irradiance value was fixed at 1000 W/m^2 and the panel temperature value was stepped up from 25 °C to 30 °C. Subsequently, the solar irradiance value was linearly decreased from 1000 W/m^2 to 800 W/m^2, and the panel temperature value was fixed at 35 °C during this state. In the fourth state, the solar irradiance value was stepped down from 800 W/m^2 to 600 W/m^2. Similarly, the panel temperature value was linearly decreased from 35 °C to 20 °C. In the fifth state, the solar irradiance value and panel temperature value were increased throughout this state. In the last state, the solar irradiance value was fixed at 1000 W/m^2, and the panel temperature value was fixed at 35 °C. Total simulation time

was 0.6 s. Extreme environmental conditions generated for this simulation are shown in Figure 10. Simulation results are given in Figure 11.

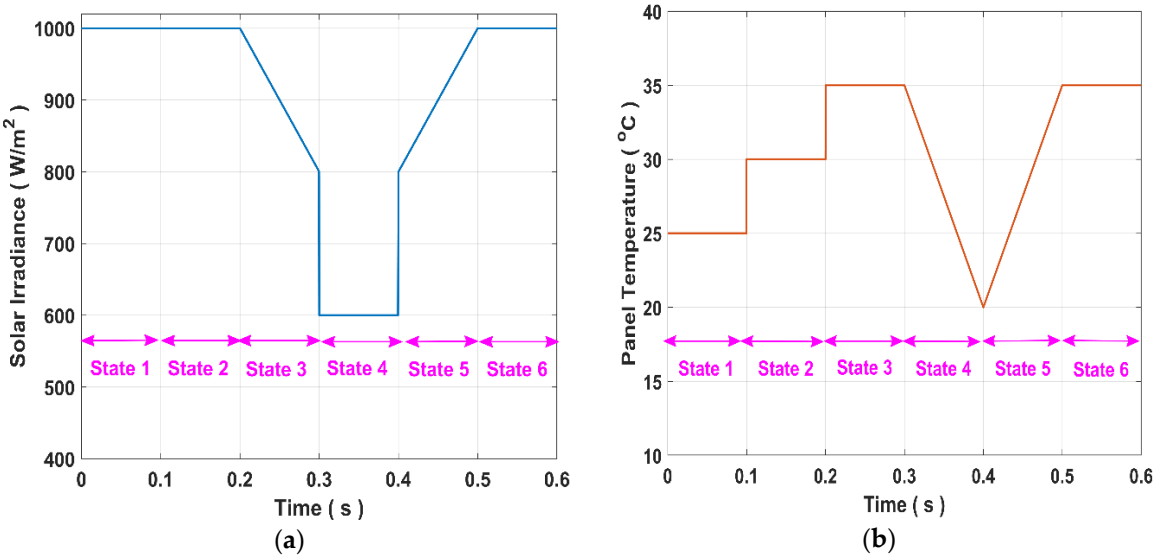

Figure 10. Extreme environmental conditions solar irradiance (**a**) panel temperature (**b**) for case 2.

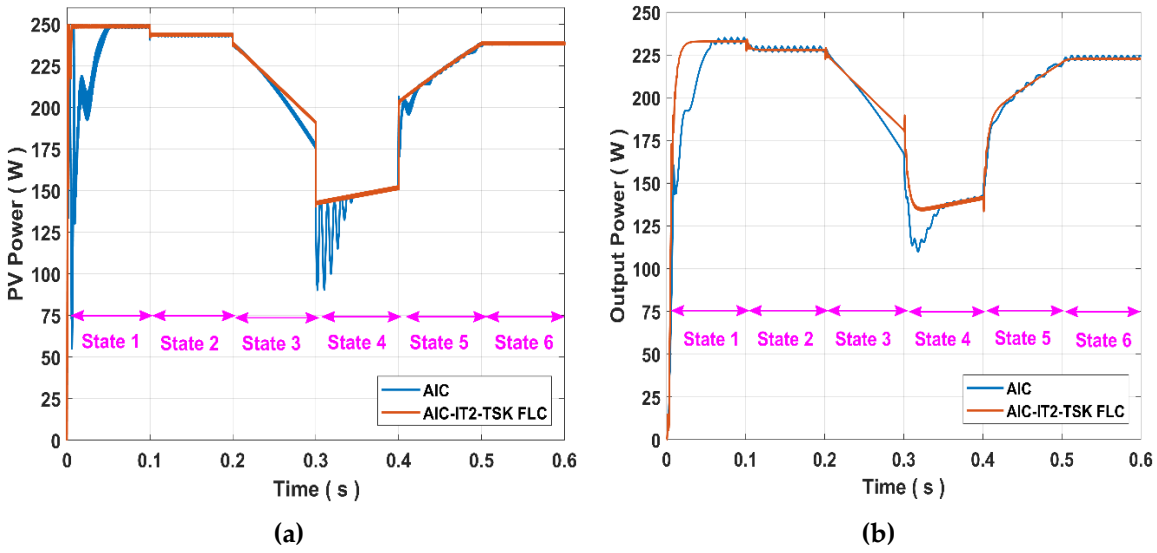

Figure 11. Output power responses of PV panel (**a**) and converter (**b**) for Case 2.

As seen in Figure 11a, in the first state, PV power with the proposed hybrid control structure is 249.4 W, while PV power with the conventional AIC MPPT method was 247.9 W. The settling times of the proposed hybrid controller and AIC MPPT method were 8 ms and 55 ms, respectively. In the second state, PV power with the AIC MPPT method was stepped down to 242.2 W and PV power with the proposed hybrid control structure was stepped down to 244.2 W. Moreover, as shown in Figure 11b, the oscillation of the output power of DC-DC converter was greatly reduced by the proposed hybrid controller. In addition, the conventional AIC MPPT method displayed poor MPP tracking performance and a long transient response, particularly under extreme environmental conditions. At the same time, the conventional AIC MPPT method caused more power losses compared to the proposed hybrid controller in the steady state condition for all states. Since power losses around the MPP reduce tracking accuracy, the MPP tracking accuracy of the proposed hybrid controller was better than

the conventional AIC MPPT method. Moreover, continuous oscillations that occur in steady-state conditions of converter output power were eliminated by the proposed hybrid controller.

4. Experimental Studies

In this section, the implemention of the proposed hybrid control structure using an experimental setup based on dSPACE DS1104 which can work in real time with MATLAB/Simulink environment is described. A panel that is located in the roof of a real PV plant and installed standalone was used to evaluate the performance of the proposed hybrid control structure under real environmental conditions. The real view of the PV plant and the photograph related to the experimental setup of MPPT based on AIC-IT2-TSK-FLC is shown in Figure 12. As seen in Figure 12, the part of the experimental setup marked as "1" was the interface of the ControlDesk software. The ControlDesk software was used to display the measured parameters both graphically and numerically in real-time. The other parts of experimental setup, which were a digital oscilloscope, a DC-DC boost converter, a resistor, and a PV panel are marked as "2", "3", "4", "5" in Figure 11 respectively. In addition, a schematic presentation of the experimental study is given in Figure 13.

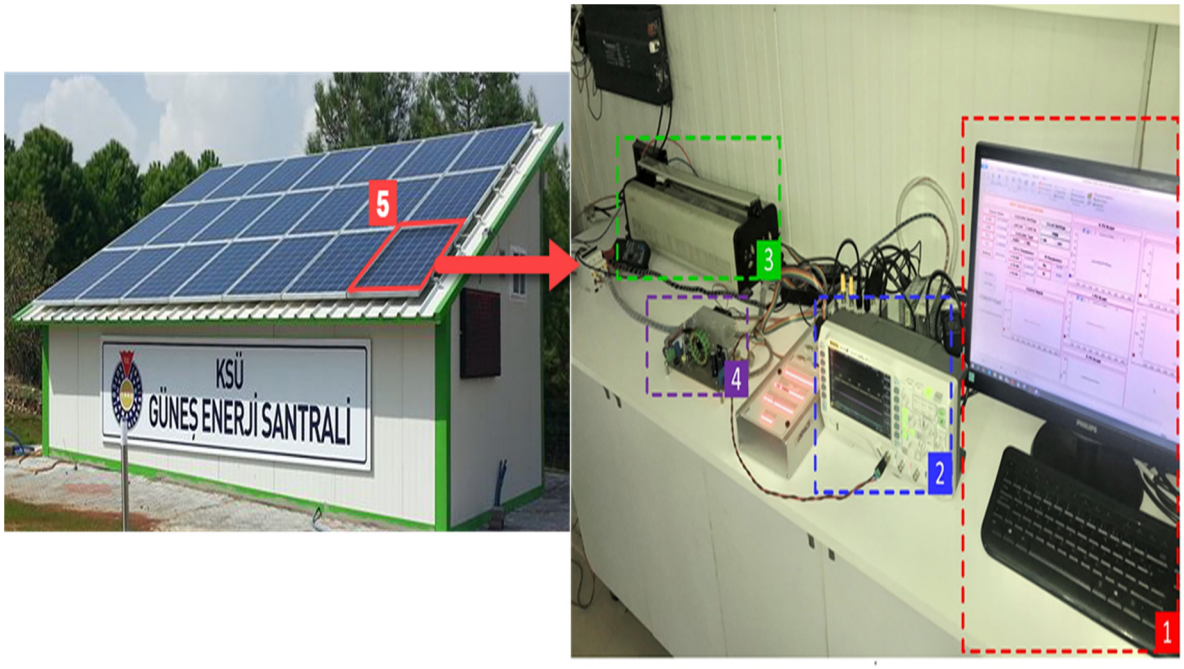

Figure 12. Experimental setup of MPPT based on AIC- IT2-TSK-FLC.

As seen in Figure 13, voltage and current sensing devices must have a high level of accuracy and sensitivity for hardware implementation of MPPT. Therefore, PICO TA018 current probe and PINTEK DP-25 voltage probes were used to measure current and voltage values of PV panel. In addition, pulse width modulation (PWM) signals received from the DS1104 control board must be amplified for switching devices. For this purpose, an isolated PWM gate driver circuit based on HCPL 3120 optocoupler was designed in the present study. This optocoupler was preferred to it has a more stable output in higher switching frequencies. The real-time interface (RTI) model designed for the experimental study is shown in Figure 14. The control algorithm required for real-time operation has been implemented by this model.

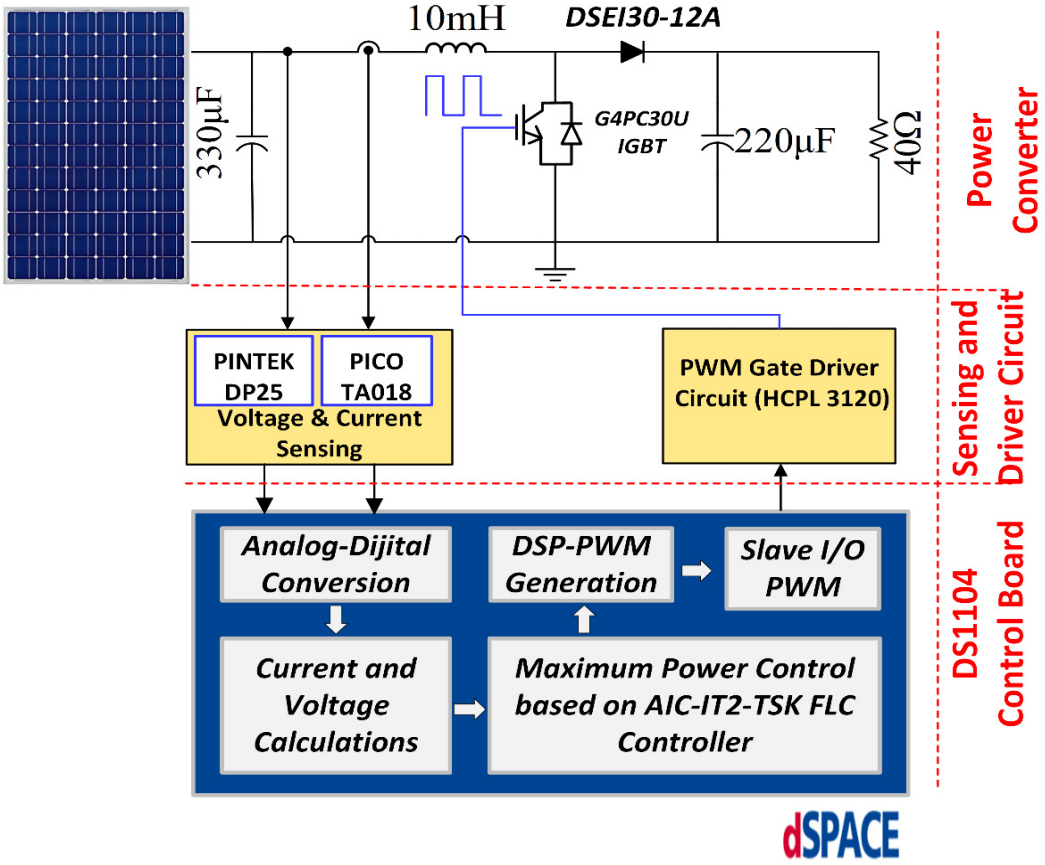

Figure 13. Schematic presentation of experimental study.

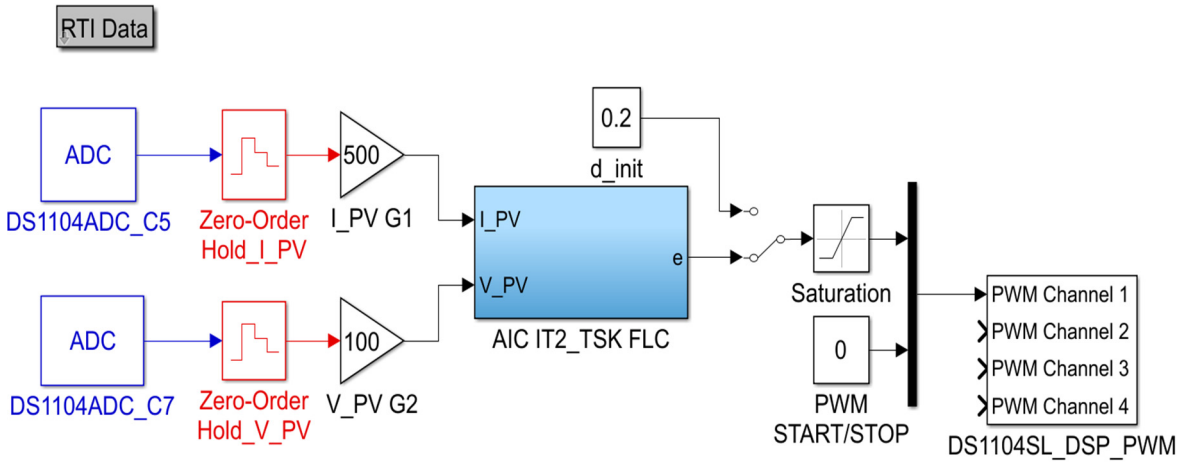

Figure 14. RTI model for proposed hybrid control structure.

As shown in Figure 14, current and voltage values of the PV panel were measured using probes and applied to analog-digital converters (ADC) of the DS1104 controller card. The current and voltage values obtained from ADC block were converted into their real values in the calibration units, and then they were applied to the 'AIC-IT2-TSKFLC' block. After the controlling process was finished, PWM signals were sent to the driver circuit. The saturation block on the RTI model was used as software protection for the duty cycle of the PWM signal. The lower and upper limits of this block were set 0.2 and 0.8 respectively. Then, these signals were applied to IGBT for the switching process. Sampling time was taken as 100 µs for the RTI model. The experimental study was performed on 25 November

2019. The solar irradiance and panel temperature values were obtained from the EVO PVI-AEC-IRR-T data logger and illustrated in Figure 15.

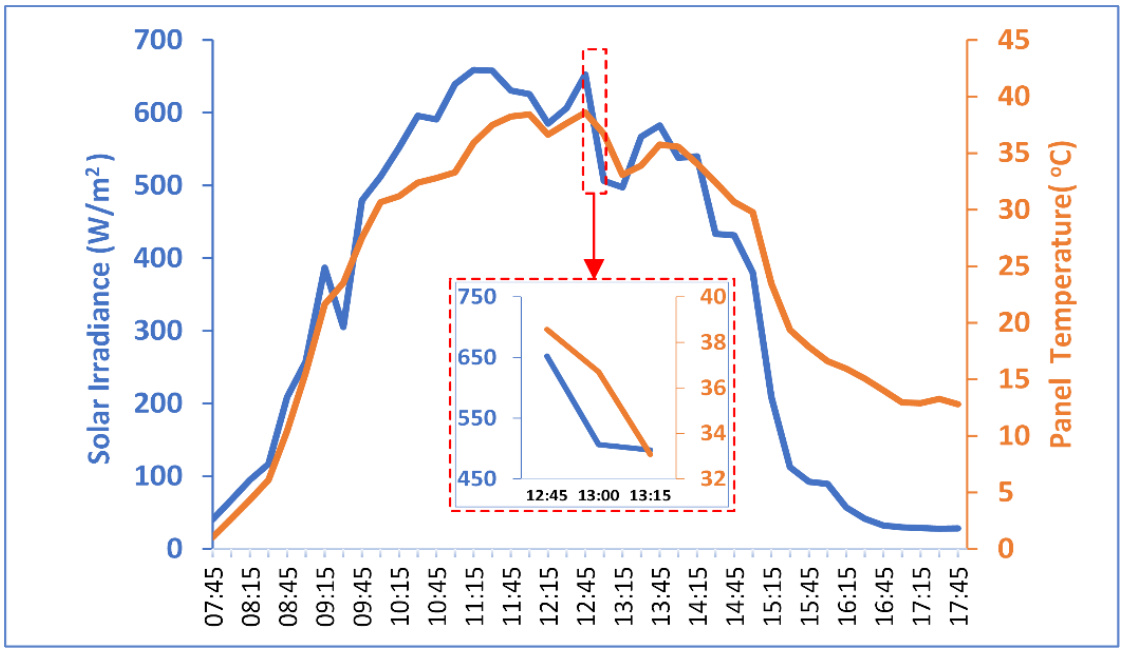

Figure 15. The actual solar irradiance and panel temperature values.

In this experimental study, the performance of the proposed hybrid control structure was analyzed to obtain maximum power from a PV panel under changes in environmental conditions between 11.45 and 12.15 h. As seen in Figure 15, the solar irradiance and panel temperature values decreased from 652.33 W/m^2 and 38.57 °C to 497.60 W/m^2 and 33.07 °C throughout the experimental operation. The PWM signal was applied to the gate driver circuit after 20.74 s of operation using the 'PWM START/STOP' block on the RTI model. Experimental results of PV voltage, PV current, PV power, control signal, and DC-DC converter output voltage (V_L) are shown in Figure 16a–e, respectively. As shown in Figure 16a, PV voltage value increased from 27.7 V to 28.61 V. Notwithstanding these environmental changes, it can clearly be seen that the proposed hybrid control structure keeps the PV voltage value almost around the MPP value. The PV current value decreased from 5.74 A to 3.61 A simultaneously with decreasing solar irradiance value. As obviously seen in Figure 16c, the power value obtained from the PV panel decreased from 165.3 W to 103.3 W, and the proposed hybrid control structure successfully decided the proper duty cycle to be applied to the DC-DC converter in order to extract maximum power from the PV panel. As seen in the control signal of the proposed hybrid control structure, despite the changes in environmental conditions, the controller generated a stable control signal for the real-time system. This situation has provided better MPP tracking performance. As seen in Figure 16e, the DC-DC converter had a stable output voltage which shows the accuracy of converter design. PV power, PV voltage, PV current, and PWM waveforms received from a digital oscilloscope are illustrated in Figure 17. The results confirm that steady-state operating performance of the AIC-IT2-TSKFLC achieves the maximum output power for the PV system.

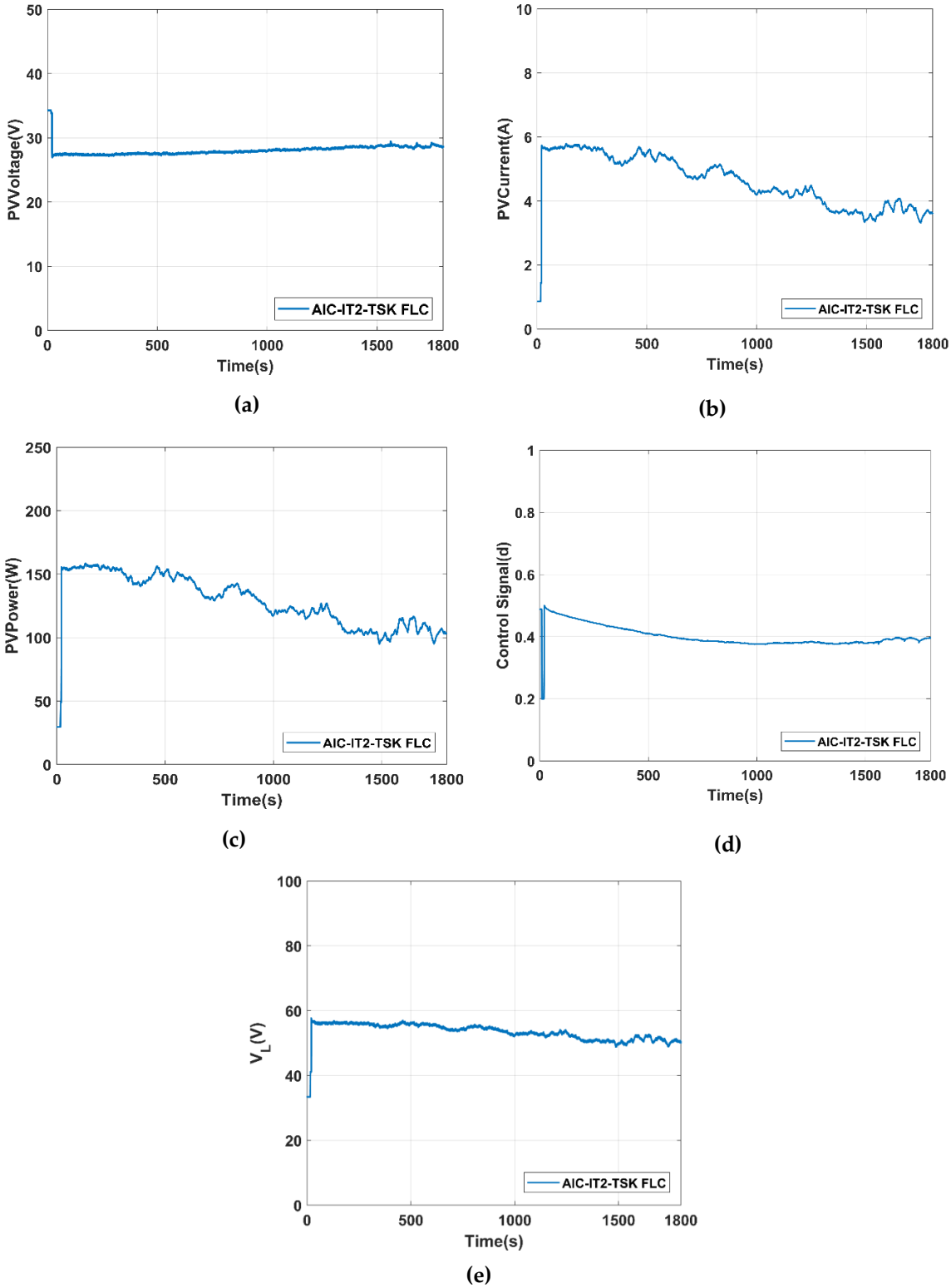

Figure 16. Experimental results of voltage (**a**), current (**b**) and power (**c**) of PV panel and control signal of AIC-IT2-TSK-FLC (**d**), output voltage of DC-DC converter (**e**).

Figure 17. Waveforms of the PV system.

5. Conclusions

This paper proposes a new hybrid MPPT method that is called AIC-IT2-TSK FLC, in order to obtain the maximum power of a PV system and reduce power fluctuations in transient and steady-state operating points. Among conventional MPPT methods, the AIC method is preferred for the hybrid MPPT controller because of a well-defined input variable with finite range, as well as a well-defined MPP operation in steady conditions. The proposed hybrid control structure consists of an effective and robust control structure that responded to changing environmental conditions and tracked MPP efficiently. The performance of the AIC-IT2-TSKFLC has been verified via simulation studies and experimental study. The results obtained from these studies demonstrate that the proposed hybrid controller successfully tracks the maximum power of the panel and provides considerable improvement in power fluctuations compared to the conventional MPPT method. These improvements contribute to reaching a stable maximum power operating point quickly for the PV system. Furthermore, the experimental results clearly indicate the validity of the proposed hybrid control structure.

Author Contributions: M.S. provide the basic idea of the research and supervise. O.F.K. researched the background literature and proposed control structure based on Interval Type-2 TSK Fuzzy Logic Controller. A.G. developed the Simulink/MATLAB model of the proposed control approach and improved existing simulation studies and commented the comparison of conventional AIC MPPT method. O.F.K. and A.G. organized and drafting of the manuscript. All authors read and approved the final manuscript.

Funding: This research received no external funding.

Acknowledgments: This work was financially supported by the Kahramanmaras Sutcu Imam University, Scientific Research Projects Unit, the project entitled "Design and Experimental Implementation of Maximum Power Point Tracking System based on Type-2 Fuzzy Logic Controller in Photovoltaic Systems" under Project No: 2017/7-203 M.

Conflicts of Interest: The authors declare no conflict of interest.

References

1. Eltawil, M.A.; Zhao, Z. MPPT techniques for photovoltaic applications. *Renew. Sustain. Energy Rev.* **2013**, *25*, 793–813. [CrossRef]
2. Sahoo, J.; Bhattacharyya, S. Adaptive PID controller with P&O MPPT algorithm for photovoltaic system. *IETE J. Res.* **2018**, *64*, 1–12.

3. Tian, Y.; Xia, B.; Xu, Z.; Sun, W. Modified asymmetrical variable step size incremental conductance maximum power point tracking method for photovoltaic systems. *J. Power Electron.* **2014**, *14*, 156–164. [CrossRef]
4. Soon, T.K.; Mekhilef, S. A fast-converging MPPT technique for photovoltaic system under fast-varying solar irradiation and load resistance. *IEEE Trans. Ind. Inform.* **2015**, *11*, 176–186. [CrossRef]
5. Dogmus, O.; Kilic, E.; Sit, S.; Gunes, M. Adaptation of optimized PID controller with PSO algorithm to photovoltaic MPPT system. *Kahramanmaraş Sütçü İmam Univ. J. Eng. Sci.* **2017**, *20*, 1–8.
6. Loukriz, A.; Haddadi, M.; Messalti, S. Simulation and experimental design of a new advanced variable step size incremental conductance MPPT algorithm for PV systems. *ISA Trans.* **2016**, *62*, 30–38. [CrossRef]
7. Liu, F.; Duan, S.; Liu, F.; Liu, B.; Kang, Y. A variable step size INC MPPT method for PV systems. *IEEE Trans. Ind. Electron.* **2008**, *55*, 2622–2628.
8. Kececioglu, O.F.; Acikgoz, H.; Gani, A. Fuzzy-PI based MPPT control for photovoltaic systems. In Proceedings of the Innovations in Intelligent Systems and Applications, Adana, Turkey, 4–6 October 2019; pp. 1–4.
9. Yilmaz, U.; Turksoy, O.; Teke, A. Improved MPPT method to increase accuracy and speed in photovoltaic systems under variable atmospheric conditions. *Int. J. Electr. Power Energy Syst.* **2019**, *113*, 634–651. [CrossRef]
10. Palaniswamy, A.M.; Srinivasan, K. Takagi-Sugeno fuzzy approach for power optimization in standalone photovoltaic systems. *Sol. Energy* **2016**, *139*, 213–220. [CrossRef]
11. Rezk, H.; Aly, M.; Al-Dhaifallah, M.; Shoyama, M. Design and hardware implementation of new adaptive fuzzy logic-based MPPT control method for photovoltaic applications. *IEEE Access* **2019**, *7*, 106427–106438. [CrossRef]
12. Ozdemir, S.; Altin, N.; Sefa, I. Fuzzy logic based MPPT controller for high conversion ratio quadratic boost converter. *Int. J. Hydrog. Energy* **2017**, *42*, 17748–17759. [CrossRef]
13. Altin, N. Interval Type-2 Fuzzy logic controller based maximum power point tracking in photovoltaic systems. *Adv. Electr. Comput. Eng.* **2013**, *13*, 65–70. [CrossRef]
14. Danandeh, M.A.; Mousavi, G.S.M. A new architecture of INC-fuzzy hybrid method for tracking maximum power point in PV cells. *Sol. Energy* **2018**, *171*, 692–703. [CrossRef]
15. Shiau, J.K.; Wei, Y.C.; Chen, B.C. A study on the fuzzy-logic-based solar power MPPT algorithms using different fuzzy input variables. *Algorithms* **2015**, *8*, 100. [CrossRef]
16. Mendel, J.M. *Uncertain Rule-Based Fuzzy Logic Systems: Introduction and New Directions*; Prentice Hall: Upper Saddle River, NJ, USA, 2001; pp. 66–69.
17. Vimalarani, C.; Kamaraj, N.; Babu, B.C. Improved method of maximum power point tracking of photovoltaic (PV) array using hybrid intelligent controller. *Optik* **2018**, *168*, 403–415.
18. Kececioglu, O.F. Robust control of high gain DC-DC converter using Type-2 Fuzzy Neural Network controller for MPPT. *J. Intell. Fuzzy Syst.* **2019**, *37*, 941–951. [CrossRef]
19. Chatterjee, A.; Chatterjee, R.; Matsuno, F.; Endo, T. Augmented stable fuzzy control for flexible robotic arm using LMI approach and Neuro-Fuzzy state space modeling. *IEEE Trans. Ind. Electron.* **2008**, *55*, 1256–1270. [CrossRef]
20. Precup, R.E.; Tomescu, M.L.; Dragos, C.A. Stabilization of Rössler chaotic dynamical system using fuzzy logic control algorithm. *Int. J. Gen. Syst.* **2014**, *43*, 413–433. [CrossRef]
21. Radgolchin, M.; Moeenfard, H. Development of a multi-level adaptive fuzzy controller for beyond pull-in stabilization of electrostatically actuated microplates. *J. Vib. Control* **2018**, *24*, 860–878. [CrossRef]
22. Gil, R.P.A.; Johanyák, Z.C.; Kovács, T. Surrogate model based optimization of traffic lights cycles and green period ratios using microscopic simulation and fuzzy rule interpolation. *Int. J. Artif. Intell.* **2018**, *16*, 20–40.
23. Haidegger, T.; Kovács, L.; Preitl, S.; Precup, R.E.; Benyó, B.; Benyó, Z. Controller design solutions for long distance telesurgical applications. *Int. J. Artif. Intell.* **2011**, *6*, 48–71.
24. Takács, Á.; Kovács, L.; Rudas, I.J.; Precup, R.E.; Haidegger, T. Models for force control in telesurgical robot systems. *Acta Polytech. Hung.* **2015**, *12*, 95–114.
25. Tai, K.; El-Sayed, A.R.; Biglarbegian, M.; Gonzalez, C.I.; Castillo, O.; Mahmud, S. Review of recent Type-2 Fuzzy controller applications. *Algorithms* **2016**, *9*, 39. [CrossRef]
26. Karnik, N.N.; Mendel, J.M.; Liang, Q. Type-2 fuzzy logic systems. *IEEE Trans. Fuzzy Syst.* **1999**, *7*, 643–658. [CrossRef]
27. Takagi, T.; Sugeno, M. Fuzzy identification of systems and its applications to modeling and control. *IEEE Trans. Syst. Man Cybern.* **1985**, *15*, 116–132. [CrossRef]

28. Liang, Q.; Mendel, J.M. Interval type-2 fuzzy logic systems: Theory and design. *IEEE Trans. Fuzzy Syst.* **2000**, *8*, 535–550. [CrossRef]
29. Wu, D. Twelve considerations in choosing between Gaussian and trapezoidal membership functions in Interval Type-2 fuzzy logic controllers. In Proceedings of the IEEE International Conference on Fuzzy Systems, Brisbane, Australia, 10–15 June 2012; pp. 1–8.
30. Kececioglu, O.F.; Gani, A.; Kilic, E.; Sekkeli, M. Dynamic performance evaluation of PI and ınterval type-2 takagi-sugeno-kang fuzzy controller on positive output luo converter. *NESciences* **2019**, *4*, 32–39.
31. Biglarbegian, M.; Melek, W.W.; Mendel, J.M. On the stability of Interval Type-2 TSK fuzzy logic control systems. *IEEE Trans. Syst. Man Cybern. B Cybern.* **2010**, *40*, 798–818. [CrossRef]